Article

Seepage Behavior of Underwater Tunnels in Stratum with Inclined Surface: Insights from Numerical Analysis

Tianjiao Zhang, Lei Huang, Dongjie Li and Yongming Wang*

Power China Huadong Engineering Co.,Ltd., Zhejiang Engineering Research·Center of Green Mine·Technology and Intelligent·Equipment, Hangzhou, 311122, China.
* Correspondence: 11712022@zju.edu.cn; Tel.: +86-18069869651

Abstract: This paper is to investigate the seepage behavior of underwater tunnel with inclined boundary at the contact between water body and underwater stratum. Extensive finite element analyses using COMSOL are performed considering various magnitudes of inclination degree of underwater soil surface. The rationality of the numerical analysis method is demonstrated via comparing with analytical solutions. It is found that the inclined boundary has a significant impact on the seepage field of underwater tunnel. The hydraulic head distribution, streamline evolution, velocity and other aspects are comprehensively analyzed, and relevant conclusions are drawn. The streamlines in waters are not vertically downward, but presents a certain acute angle distribution with the stratum direction. And the interface angle toward the depth is larger. Streamlines will also become denser. The streamline flows into the tunnel from all directions. And the attenuation speed of water head in the lower part of tunnel is less than that in the upper part. Thereby serving the optimal design and construction of practical projects.

Keywords: Underwater tunnel; Seepage field; Obique boundary; Numerical simulation

1. Introduction

The first underwater tunnel in the world appeared in the Euphrates River of Babylon in over 2000 BC. In the 1840s, the first modern underwater tunnel was built, which across the

Thames River. Since 1930s, the establishment of underwater tunnels goes to a climax. In the past half century, the whole number of underwater tunnels existing in the world was about the sum of the previous several centuries. However, compared with the fast establishment of underwater tunnels, the theoretical development of underwater tunnel is only in the initial stage. How to extract scientific problems from engineering problems and analyze them qualitatively and quantitatively is a problem worth considering, and how to hold the major conflicts are the key factors in the theoretical study of underwater tunnels.

The first try of mankind was in 1960s, when Harr[1] used the mirror method to deal with problems for the first time, which transfered the method of dealing with electromagnetic field to geotechnical engineering. Subsequently, the mirror image method aroused the interest of the academic circles. The more classical ones were Fernandez[2], Lei[3]and Joo[4]. The latter simplified the lining to the boundary of equal liquid energy, taking the classical Goodman solution [5] as basis. Some other methods also occured. Bobet[6-7] studied the lining stress field without water, which laid a foundation for tunnel response under different seepage conditions.

Polubarinova-Kochina[8] obtained an approximate function for the seepage of the circular tunnel according to the hypothesis that the inflow condition around the hole is at a stable state. Zhang and Franklin[9] obtained a combined solution, which was suitable for the prediction of ubiquitous water inflows. Su et al.[10] studied semi-analytical solutions for evaluating groundwater location and the number of water inflow in tunnel. Ying et al.[11] researched the response of waves on seepage field. Zareifard[12] studied the seepage of tunnel under the boundary of cracked lining structure.

In recent years, as an effective method to deal with semi-infinite boundary problems, the conformal mapping method of complex variable functions has gradually developed. EL Tani[13] used conformal mapping method to solve the seepage field of tunnel inner wall under zero water pressure. Kolymbas[14] assumed equal liquid energy at the outside boundary of the lining, and the theoretical solution of tunnel seepage problem was obtained by the complex variable function. As a result of using conformal mapping method, Park et al.[15] mapped the semi-infinite seepage region into different forms of seepage area, and considered several boundary conditions to obtain theoretical solutions in some special conditions. Conformal mapping method is a theoretical method of complex variable function. However, in the face of irregular boundary, the selection of conformal transformation function will pose a problem. For example, due to the heterogeneity of geotechnical engineering, multi-layer soil will contain inner boundary. Hu et al.[16] researched the shield tunnel in heterogeneous media, and found that the interface of the media had much influence. Rieckh et al.[17] obtained a tunnel boundary element model in anisotropic multilayer media. Zhang et al. [18] researched the influence of the deformation of multi-layer media on the tunnel. Khezri et al. [19] studied the lowest supporting pressure of tunnel in multi-layer media. Huang et al.[20] obtained the response of multi-layer soil to moving load. And more theoretical and practical contributions in the academic field[21-32].

However, there are few studies on seepage problems facing complex boundaries. Conformal transformation method is complex and not applicable to complex boundary calculation, and

it is applicable to semi-infinite space with horizontal boundary. In the long sedimentary history of soil, the heterogeneity is first manifested in the non-level of underwater soil interface. In order to be applicable to more practical engineering situation, this paper attempts to study non-horizontal seepage boundary in finite field.

2. Materials and Methods

2.1 Tunnel physical model

Fig.1 shows the whole physical model of the underwater tunnel to describe the engineering problem. In this paper, for the high efficiency of deduction, the $(0,0)$ of coordinate system is set on the surface of the top soil. The underwater soil layer is distributed obliquely. The dip angle of the stratum is θ. The permeability coefficient of soil is K_s. Water depth directly above the tunnel is H, and tunnel buried depth is h_b. The radius of tunnel is r. The distance between the tunnel and the impermeable boundary at the bottom is h_c. The whole area is expressed in a polar coordinate, the polar axis is expressed as φ_n, and the angle is written as β_n.
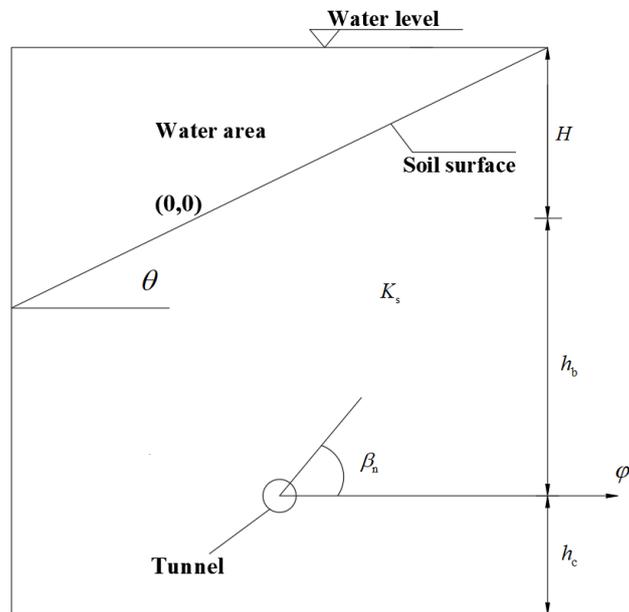
Fig.1 Physical model of the underwater tunnel

2.2 Model assumptions

The model calculated in this paper is based on the four assumptions as follows,which can make the problem be simplified reasonably.

(i)The soil is isotropic media.

(ii)The tunnel is circular and located in the finite space.

(iii)The seepage field is stable and conforms to Darcy's law.

3. Numerical Analysis of Seepage Field

3.1 Establishment of numerical model

COMSOL is used to establish the numerical calculating model. Fig.2 shows the size of the calculation case and the mesh division condition. The width of calculation area is 100m. The radius of tunnel is 5.15m, and the coordinate of the tunnel center is (50,50). The total height of the model is 200m, and the deepest depth of the water area is 100m. The left boundary of the water area is the impervious boundary. The left boundary of soil is set as permeable boundary. The right boundary of soil is set as impervious boundary. The pore water pressure at the tunnel position is 0 as outlet boundary, and the bottom boundary is regarded as impervious boundary. Soil permeability coefficient is taken as 1×10^{-8} m/s. The total number of grid cells is 843. Among them, the number of vertex elements is 8 and the number of boundary elements is 77. Firstly, it is assumed that the formation inclination angle is 45 degrees.
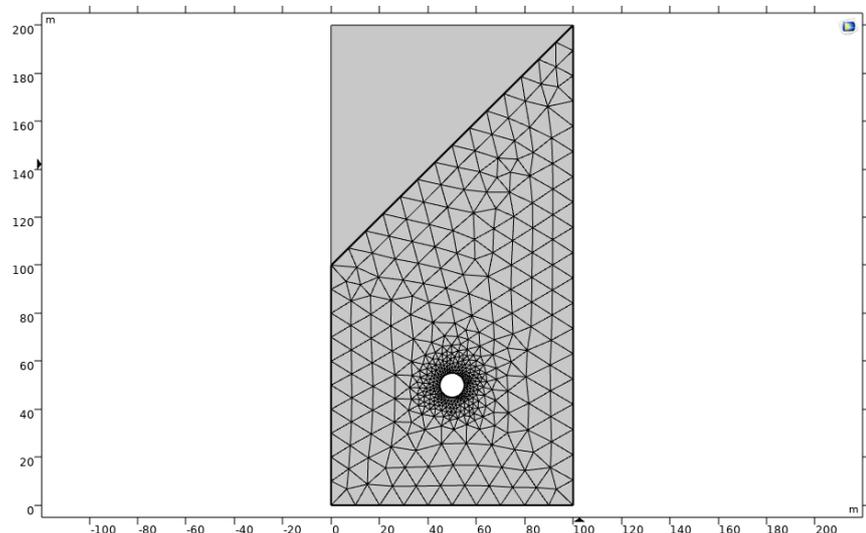
Fig.2 Mesh division of model

3.2 Results of numerical simulation

Apply a hydraulic head of 80m to the model, we can obtain the hydraulic head distribution, which is shown in Fig.3.
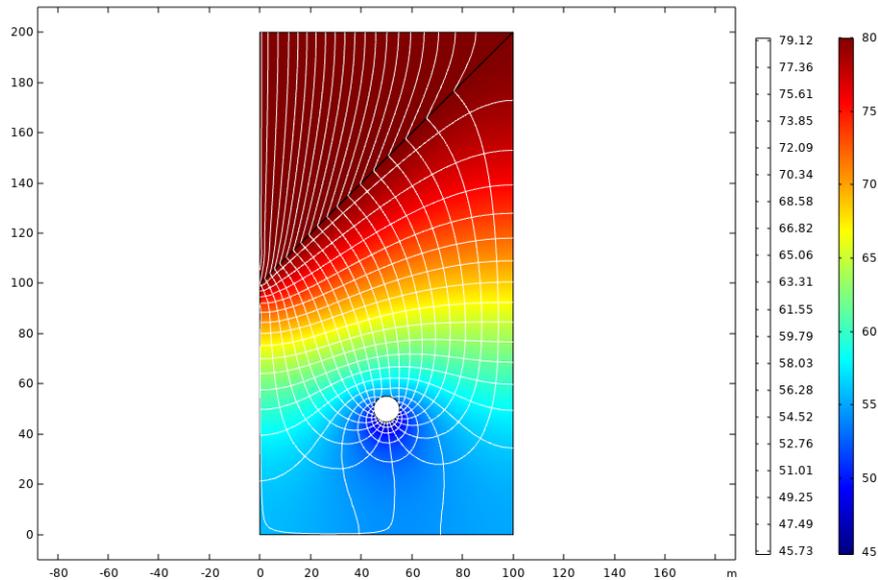
Fig.3 Hydraulic head distribution of the model

It can be seen that the streamlines in waters are not vertically downward, but presents a certain acute angle distribution with the stratum direction in Fig.3. And the interface angle toward the depth is larger. Streamlines will also become denser. Streamlines located high on the interface of inclined soil layer often have a greater degree of bending. Moreover, at the oblique interface position, the streamline turns. The angle between streamline in water and the interface of inclined soil layer is smaller than that between streamline in soil. However, the difference between the two included angles gradually decreases towards the depth of the interface. When the water flow just enters the soil layer, the water head shows strong heterogeneity. In the deep part of the oblique interface, the water head decays sharply, while in the shallow part, although it passes through more soil layers, the water head decays slowly, and the decay also presents strong nonlinearity. Between the shallow soil layer and half the tunnel depth, the angle between the water head isoline and the horizontal direction decreases with the increase of the depth. In the soil above the tunnel, the water head presents an inverted saddle distribution. Finally, the streamline flows into the tunnel from all directions. And the attenuation speed of water head in the lower part of tunnel is less than that in the upper part. And we can see the distribution of fluid velocity in soil in Fig.4.
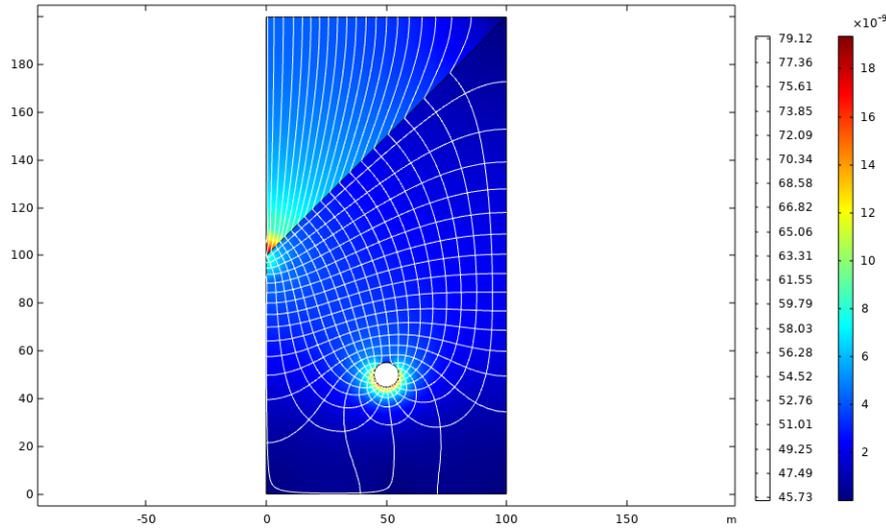
Fig.4 Fluid velocity distribution of the model

In Fig.4, We can see that there are two areas where large velocity is concentrated, one is the deepest part of the inclined stratum, and the other is the middle and lower part of the tunnel. There is a very interesting phenomenon at the oblique interface. Driven by gravity potential energy and water head, the movement of water flow in the waters presents two trends: on the one hand, it slides down the slope, on the other hand, it seeps into the inclined soil layer. The velocity of water flowing downward in the deepest part of the slope reaches the maximum, but it begins to decay rapidly after entering the lower soil layer, and the water head is even smaller than the velocity after energy attenuation due to seepage at the same depth. On the one hand, because the area with large velocity is relatively small compared with the surrounding area, the velocity is easy to dissipate; on the other hand, the velocity in the soil layer is relatively uniform, and the difference decreases gradually before entering the tunnel. However, when the water flows into the tunnel, the velocity increases sharply, which is consistent with the continuity of flow. When the flow is constant and the cross-section decreases gradually, the velocity increases sharply, which is also well reflected here.

4. Verification of Numerical Results

In order to verify the correctness and rationality of the numerical solution, analytic derivation is adopted for the same model. Firstly, the Laplace equation satisfied by the flow field is given.

$$\frac{\partial^2 H_s}{\partial x^2} + \frac{\partial^2 H_s}{\partial y^2} = 0 \qquad (1)$$

In which, H_s is the total hydraulic head in seepage field.

The general solution of the Laplace equation satisfies Fourier form is:

$$H_s = C_1 + C_2 \ln \varphi_n + \sum_{u=1}^{\infty}\left[\left(C_3 \varphi_n^{\,u} + C_4 \varphi_n^{\,-u}\right)\cos u\beta_n\right] \qquad (2)$$

The equation of inclined boundary can be written as

$$\varphi_n = \frac{h_b}{\sin \beta_n - \tan \theta \cdot \cos \beta_n} \tag{3}$$

So the hydraulic head distribution on the boundary can be expressed as

$$H_s = H - \tan \theta \cdot \varphi_n \cdot \cos \beta_n \tag{4}$$

The hydraulic gradient in polar coordinate system can be expressed as

$$i = -\left(\frac{\partial \psi_s}{\partial \varphi_n} \overrightarrow{e_{\varphi_n}} + \frac{1}{\varphi_n} \frac{\partial \psi_s}{\partial \beta_n} \overrightarrow{e_{\beta_n}} \right) \tag{5}$$

The right boundary equation can be expressed as

$$\varphi_n \cdot \cos \beta_n = L \tag{6}$$

The right boundary is impermeable, so the flow velocity v_s is 0.

Tunnel boundary:

$$\varphi_n = r \tag{7}$$

The pore pressure at the boundary is 0, then

$$H_s - \varphi_n \sin \beta_n = 0 \tag{8}$$

The lower boundary equation can be written as

$$\varphi_n \cdot \sin \beta_n = -h_c \tag{9}$$

Combining the general solution and boundary conditions, the following equations can be obtained:

$$\left\{\begin{array}{l} H - \tan\theta \cdot \varphi_n \cdot \cos\beta_n = C_1 + C_2 \ln \dfrac{h_b}{\sin\beta_n - \tan\theta \cdot \cos\beta_n} \\[2em] \quad + \displaystyle\sum_{u=1}^{\infty}\left\{\left[C_3\left(\dfrac{h_b}{\sin\beta_n - \tan\theta \cdot \cos\beta_n}\right)^{u} + C_4 \dfrac{1}{\left(\dfrac{h_b}{\sin\beta_n - \tan\theta \cdot \cos\beta_n}\right)^{u}}\right]\cos u\beta_n\right\} \\[3em] k_s\sqrt{\left(\dfrac{\partial\left\{C_1 + C_2 \ln\dfrac{L}{\cos\beta_n} + \sum_{u=1}^{\infty}\left[\left(C_3\varphi_n^{u} + C_4\varphi_n^{-u}\right)\cos u\beta_n\right]\right\}}{\partial\left(\dfrac{L}{\cos\beta_n}\right)}\right)^2 + \left(\dfrac{\cos\beta_n}{L}\dfrac{\partial\psi_s}{\partial\beta_n}\right)^2} = 0 \\[3em] k_s\sqrt{\left(\dfrac{\partial\left\{C_1 + C_2 \ln\varphi_n + \sum_{u=1}^{\infty}\left[\left(C_3\varphi_n^{u} + C_4\varphi_n^{-u}\right)\cos u\beta_n\right]\right\}}{\partial\left(-\dfrac{h_c}{\sin\beta_n}\right)}\right)^2 + \left(\dfrac{\sin\beta_n}{h_c}\dfrac{\partial\psi_s}{\partial\beta_n}\right)^2} = 0 \\[3em] \varphi_n\sin\beta_n = C_1 + C_2 \ln r + \displaystyle\sum_{u=1}^{\infty}\left\{\left[C_3 r^{u} + C_4\dfrac{1}{r^{u}}\right]\cos u\beta_n\right\} \end{array}\right. \tag{10}$$

The undetermined coefficient C_1, C_2, C_3, C_4 can be solved, and the expressions of undetermined coefficients are as follows:

$$C_1 = \frac{A_2(B_2 K_3 - B_3 K_2) + A_1(B_2 D_3 K_4 - B_2 D_4 K_3 - B_3 D_2 K_4 + B_3 D_4 K_2 + B_4 D_2 K_3 - B_4 D_3 K_2)}{B_1(D_2 K_3 - D_3 K_2) - B_2(D_1 K_3 - D_3 K_1 + D_3 K_4 - D_4 K_3) + B_3(D_1 K_2 - D_2 K_1 + D_2 K_4 - D_4 K_2) - B_4(D_2 K_3 - D_3 K_2)}$$

$$C_2 = \frac{A_2(B_1 K_3 - B_3 K_1 + B_3 K_4 - B_4 K_3) + A_1(B_1 D_3 K_4 - B_1 D_4 K_3 - B_3 D_1 K_4 + B_3 D_4 K_1 + B_4 D_1 K_3 - B_4 D_3 K_1)}{B_1(D_2 K_3 - D_3 K_2) - B_2(D_1 K_3 - D_3 K_1 + D_3 K_4 - D_4 K_3) + B_3(D_1 K_2 - D_2 K_1 + D_2 K_4 - D_4 K_2) - B_4(D_2 K_3 - D_3 K_2)}$$

$$C_3 = \frac{A_2(B_1 K_2 - B_2 K_1 + B_2 K_4 - B_4 K_2) + A_1(B_1 D_2 K_4 - B_1 D_4 K_2 - B_2 D_1 K_4 + B_2 D_4 K_1 + B_4 D_1 K_2 - B_4 D_2 K_1)}{B_1(D_2 K_3 - D_3 K_2) - B_2(D_1 K_3 - D_3 K_1 + D_3 K_4 - D_4 K_3) + B_3(D_1 K_2 - D_2 K_1 + D_2 K_4 - D_4 K_2) - B_4(D_2 K_3 - D_3 K_2)}$$

$$C_4 = \frac{A_2(B_2 K_3 - B_3 K_2 + B_2 K_4 - B_4 K_2) + A_1(B_1 D_2 K_3 - B_1 D_3 K_2 - B_2 D_1 K_3 + B_2 D_3 K_1 + B_3 D_1 K_2 - B_3 D_2 K_1)}{B_1(D_2 K_3 - D_3 K_2) - B_2(D_1 K_3 - D_3 K_1 + D_3 K_4 - D_4 K_3) + B_3(D_1 K_2 - D_2 K_1 + D_2 K_4 - D_4 K_2) - B_4(D_2 K_3 - D_3 K_2)}$$

In which,

$$B_1 = \ln\frac{h_b}{\sin\beta_n - \tan\theta \cdot \cos\beta_n}, \qquad B_2 = \frac{\partial\ln\dfrac{L}{\cos\beta_n}}{\partial\left(\dfrac{L}{\cos\beta_n}\right)}, \qquad B_3 = \frac{\partial\ln\varphi_n}{\partial\left(-\dfrac{h_c}{\sin\beta_n}\right)}, \qquad B_4 = \ln r,$$

$$K_1 = \sum_{u=1}^{\infty}\left(\frac{h_b}{\sin\beta_n - \tan\theta \cdot \cos\beta_n}\right)^{u}\cos u\beta_n, \qquad K_2 = \frac{\partial\left(\sum_{u=1}^{\infty}\varphi_n^{u}\cos u\beta_n\right)}{\partial\left(\dfrac{L}{\cos\beta_n}\right)}, \qquad K_3 = \frac{\partial\left(\sum_{u=1}^{\infty}\varphi_n^{u}\cos u\beta_n\right)}{\partial\left(-\dfrac{h_c}{\sin\beta_n}\right)},$$

$$K_4 = \sum_{u=1}^{\infty} r^u \cos u\beta_n \quad , \qquad D_1 = \sum_{u=1}^{\infty} \frac{1}{\left(\dfrac{h_b}{\sin\beta_n - \tan\theta \cdot \cos\beta_n} \right)^u} \cos u\beta_n \quad , \qquad D_2 = \frac{\partial\left(\sum_{u=1}^{\infty} \dfrac{\cos u\beta_n}{\varphi_n^{\,u}} \right)}{\partial\left(\dfrac{L}{\cos\beta_n} \right)} \quad ,$$

$$D_3 = \frac{\partial\left(\sum_{u=1}^{\infty} \dfrac{\cos u\beta_n}{\varphi_n^{\,u}} \right)}{\partial\left(-\dfrac{h_c}{\sin\beta_n} \right)} \quad , \qquad D_4 = \sum_{u=1}^{\infty} \left(\frac{\cos u\beta_n}{r^u} \right)$$

Substitute specific numerical values according to the example model, and compare with the numerical results, as shown in Fig.5. Taking the head distribution of the left and right vertical lines of the tunnel for analysis, we can see that they are highly consistent, thus verifying the correctness and rationality of the numerical solution.
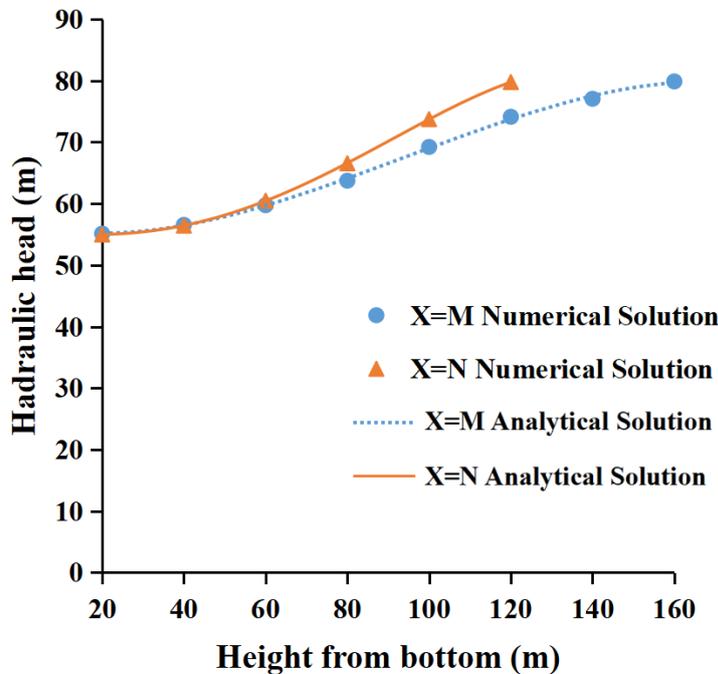
Fig.5 Comparison between analytical solution and numerical results

5. Parametric Analysis

In practical engineering, the inclination degree of underwater soil surface is different. This paper studies the influence of different stratum inclination angles on seepage field, and provides reference for practical engineering construction. Change the inclination angle of the upper boundary, and take the inclination angles of 15 degrees, 30 degrees, 60 degrees and 75 degrees to study the response of seepage field. Fig.6 to Fig.9 show the hydraulic head distribution at different angles.
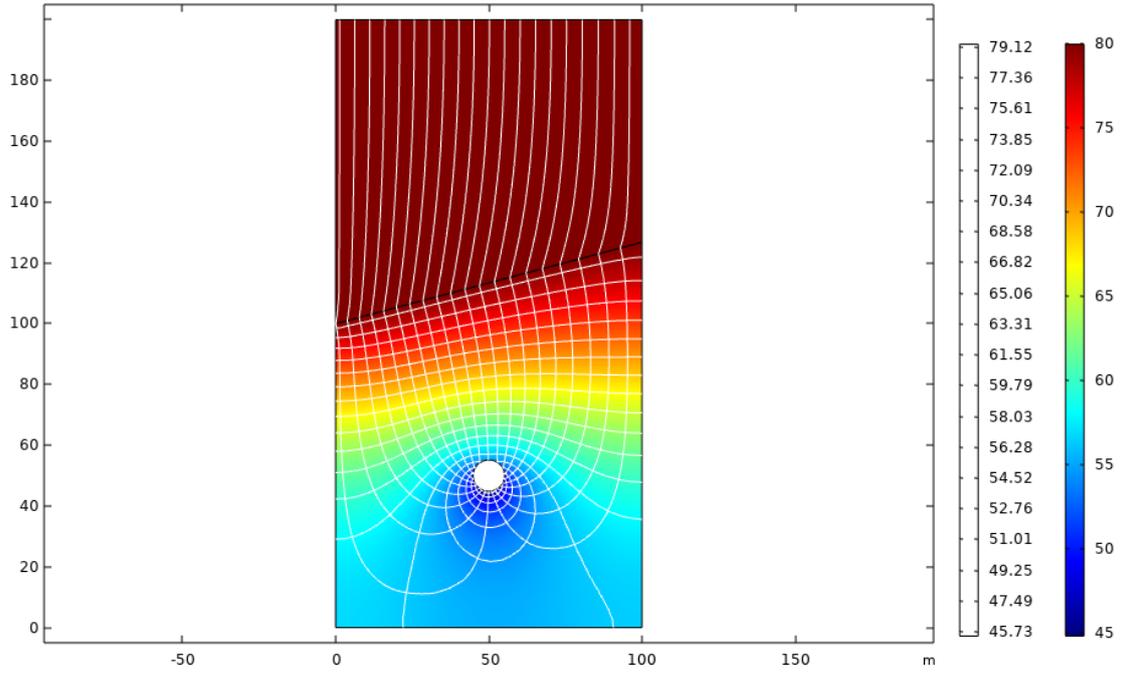
Fig.6 Hydraulic head distribution when the slope angle of soil surface is 15 degrees
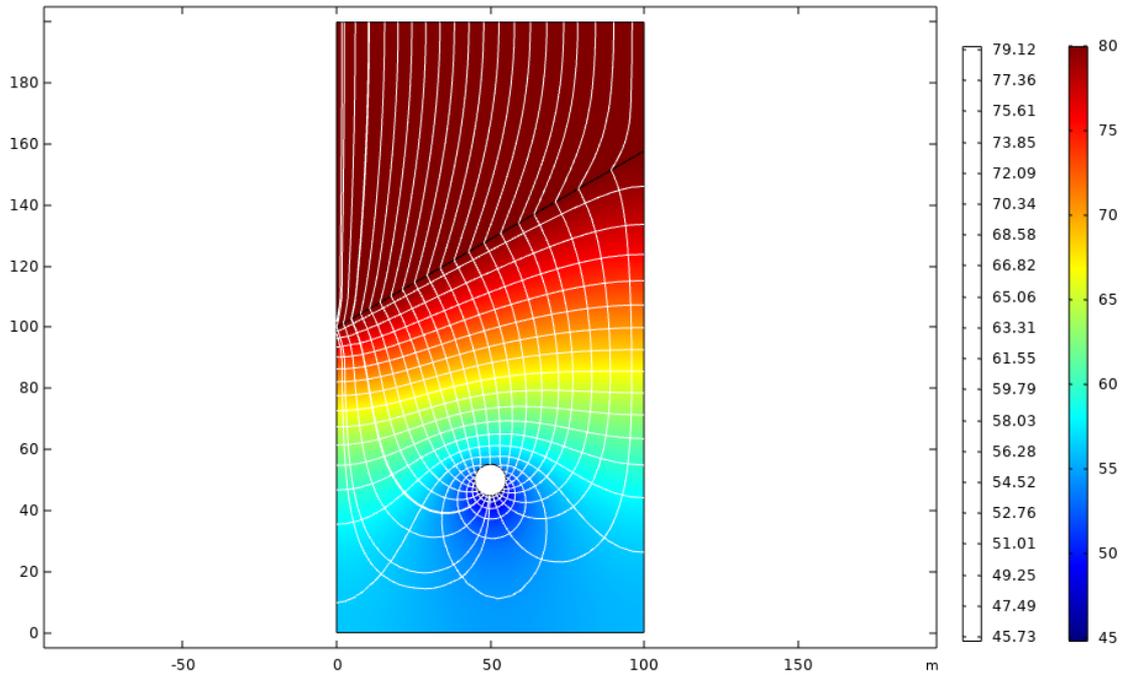
Fig.7 Hydraulic head distribution when the slope angle of soil surface is 30 degrees
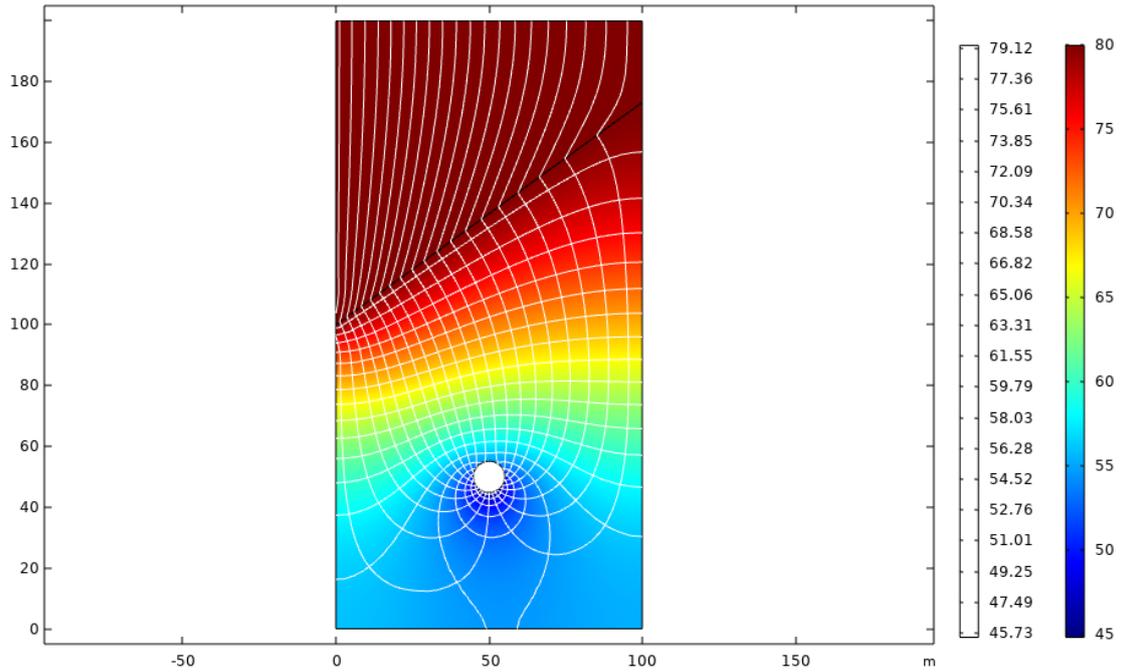
Fig.8 Hydraulic head distribution when the slope angle of soil surface is 60 degrees
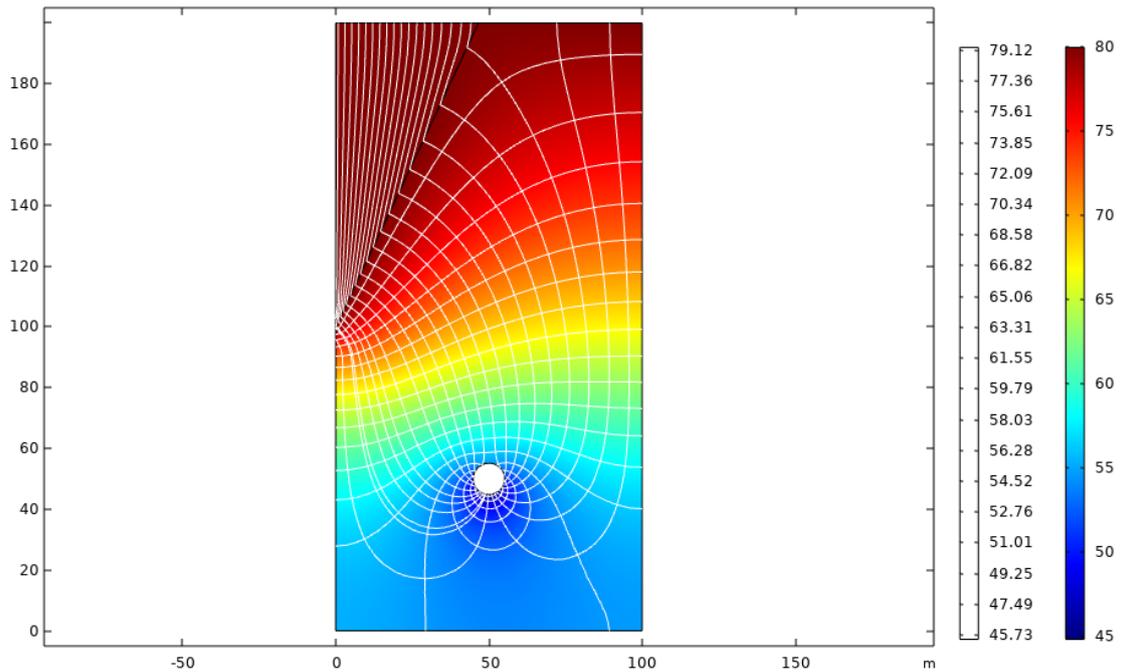
Fig.9 Hydraulic head distribution when the slope angle of soil surface is 75 degrees

According to Fig.6 to Fig.9, it can be seen that with the change of formation inclination angle, the hydraulic head distribution has a certain change, which is most obviously reflected in the change of streamline. When the inclination angle is 15 degrees, the streamline tends to be vertically distributed, and the acute angle between the streamline and the formation surface is also very large. The angle between the streamlines in the water area and the oblique interface of the soil layer gradually increases with the increase of the interface depth. Up to half the buried depth, the head loss is almost linearly distributed with the depth, however, down to half the buried depth, the head loss is obviously nonlinear. It is distributed in inverted saddle shape above the tunnel. With the gradual increase of inclination angle, the distribution of this

inverted saddle shape is gradually smooth. And the nonlinearity of head loss in shallow soil layer is gradually obvious. The response of flow velocity field to the change of dip angle is shown in Fig.10 to Fig.13.
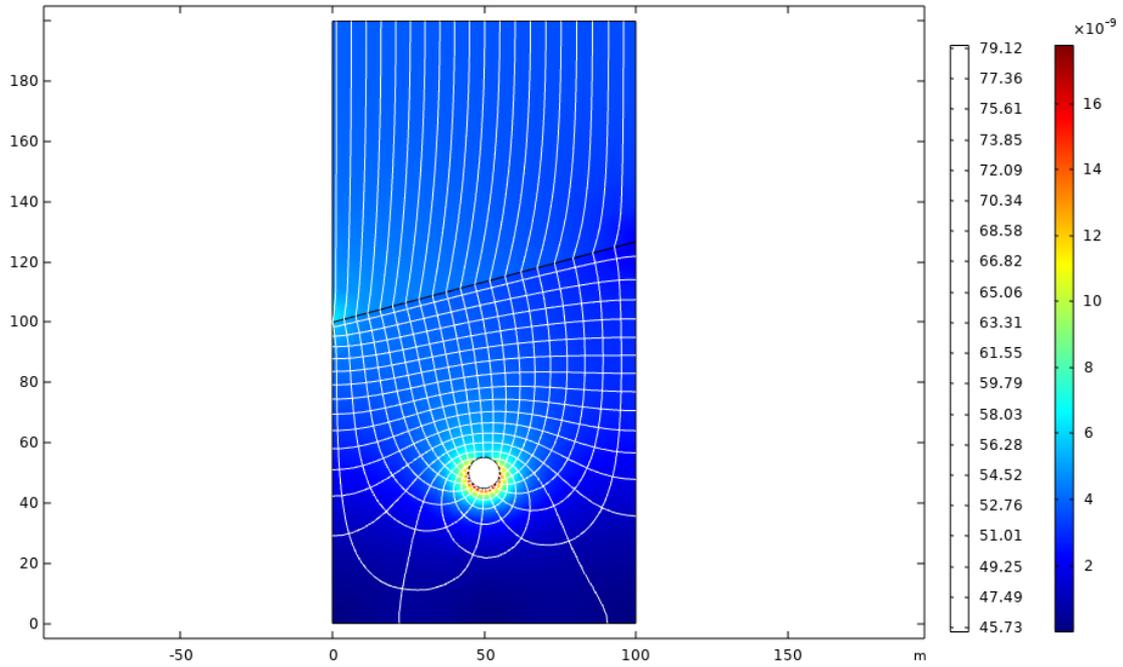
Fig.10 Flow velocity distribution when the slope angle of soil surface is 15 degrees
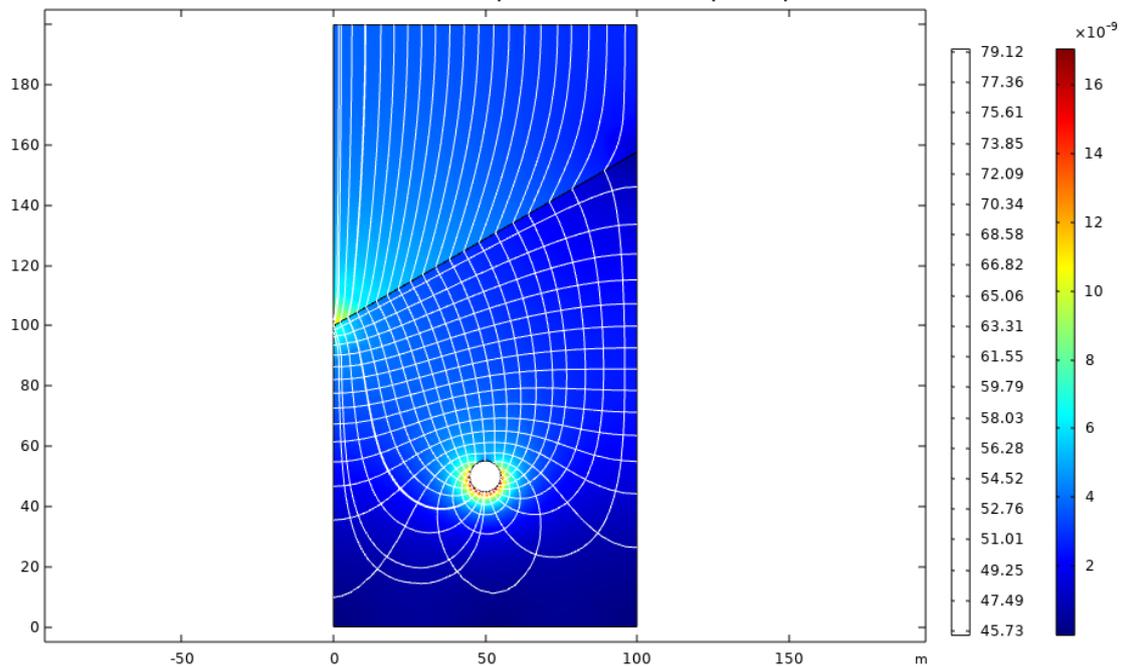
Fig.11 Flow velocity distribution when the slope angle of soil surface is 30 degrees
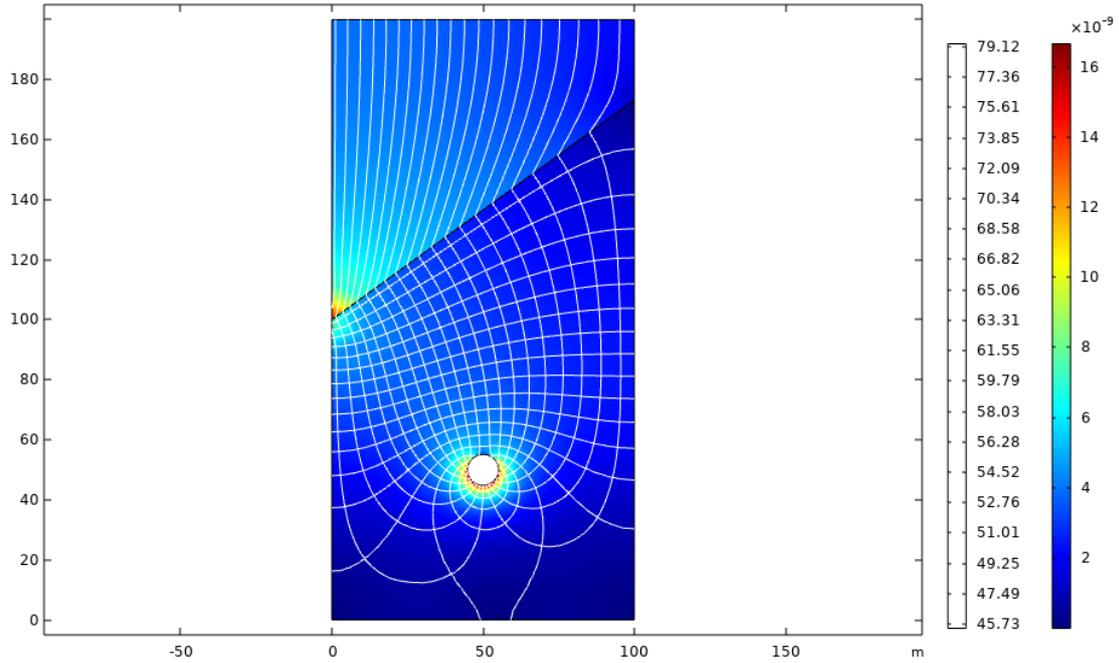
Fig.12 Flow velocity distribution when the slope angle of soil surface is 60 degrees
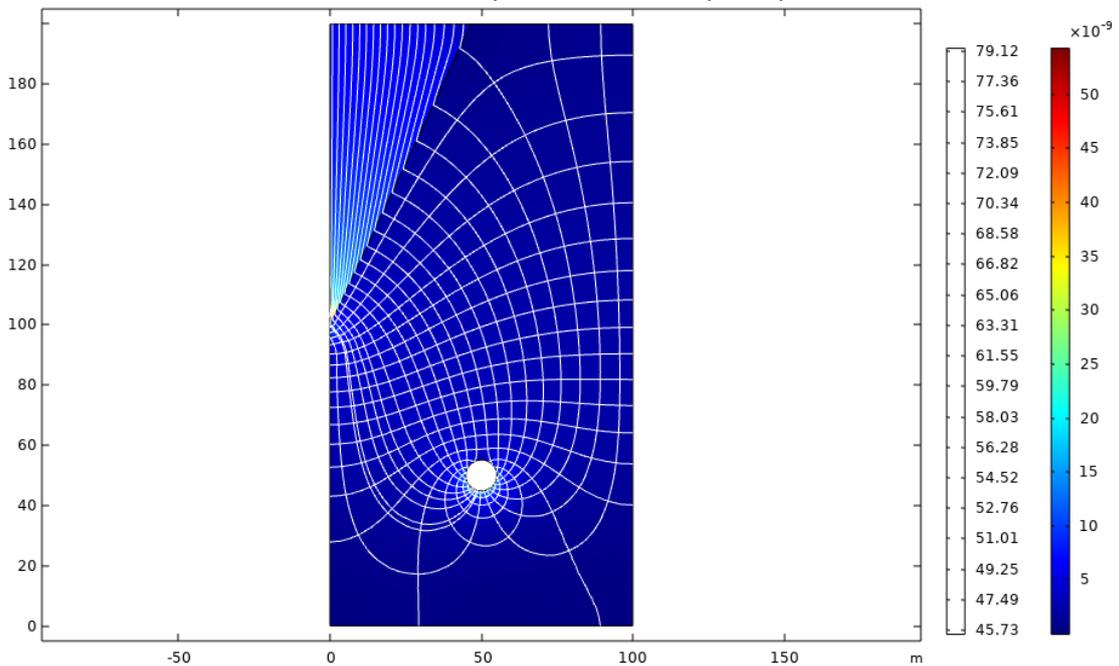
Fig.13 Flow velocity distribution when the slope angle of soil surface is 75 degrees

According to Fig.10 to Fig.13, when the inclined angle of underwater stratum boundary is 15 degrees and 30 degrees, the increase of flow velocity in the deepest part of the inclined boundary is not particularly obvious, but when the angle is 60 degrees, the flow velocity at this position increases significantly, but when the angle becomes 75 degrees, the flow velocity in the deepest part of the interface decreases significantly. This is because the convergence of velocity is not obvious when the inclination angle of the stratum is small, but the velocity increases sharply when the inclination angle of the stratum increases further. However, when the inclination angle continues to increase, the fluid in the water area is

Eng. Solut. Mech. Mar. Struct. Infrastruct., 2024, Vol. 1, Issue 1

14 of 16

mainly seepage, and the flow on the interface is not the main movement trend, so the velocity in the deepest part of the interface will not be too large. This can be used for reference in practical engineering construction and optimization design.

6. Discussion

When the hydraulic seepage boundary is inclined, it can be seen that the seepage field is different from the traditional seepage energy distribution, because the inclined boundary surface will cause energy accumulation, and the greater the inclination angle, the more energy accumulation will have a great influence on the pore pressure and velocity around the hole, resulting in extremely uneven distribution of pore pressure and velocity around the hole. In practical engineering, targeted waterproof measures should be taken for safety. For example, when the inclination angle of the inclined surface is small, The middle part is the place where the tunnel velocity is high, so the waterproof design should be strengthened here. When the inclination angle is slightly large and relatively large, the places where the tunnel velocity is high are the lower part and the bottom part, so the waterproof design and waterproof measures during construction should be followed up, which is safer.

7. Conclusions

Inclined stratum has significant influence on water head, streamline and velocity. The streamlines in waters are not vertically downward, but presents a certain acute angle distribution with the stratum direction. And the interface angle toward the depth is larger. Streamlines will also become denser.

The angle between streamline in water and the interface of inclined soil layer is smaller than that between streamline in soil. However, the difference between the two included angles gradually decreases towards the depth of the interface.

When the water flow just enters the soil layer, the hydraulic head shows strong heterogeneity. In the deep part of the oblique interface, the water head decays sharply, while in the shallow part, although it passes through more soil layers, the water head decays slowly, and the decay also presents strong nonlinearity.

The streamline flows into the tunnel from all directions. And the attenuation speed of water head in the lower part of tunnel is less than that in the upper part.

When the inclination angle is small, the streamline tends to be vertically distributed, and the acute angle between the streamline and the formation surface is also very large. The angle between the streamlines in the water area and the oblique interface of the soil layer gradually increases with the increase of the interface depth.

With the gradual increase of inclination angle, the distribution of this inverted saddle shape is gradually smooth. And the nonlinearity of head loss in shallow soil layer is gradually obvious.

References

1. Harr, M. E. Groundwater and Seepage. Soil science, 1962, 95(4):289. Doi:10.1097/00010694-196304000-00040

2. G.Fernandez & T.A. Alvarez Jr. Seepage-induced effective stresses and water pressures around pressure tunnels: Journal of Geotechnical Engineering — ASCE, 120(1), 1994. Doi:10.1016/0148-9062(94)91263-7

3. S. Lei, An analytical solution for steady flow into a tunnel, Ground Water, vol. 37, no. 1, pp. 23–26, 1999. Doi:10.1186/1752-153X-7-176

4. Joo E J , Shin J H . Relationship between water pressure and inflow rate in underwater tunnels and buried pipes. Géotechnique, 2013, 64(3):226-231. Doi:10.1007/s40279-014-0211-9

5. GOODMAN R E, MOYE D G, VAN SCHALKWYK A et al. Groundwater inflows during tunnel driving. Engineering Geology. 1965, 2(1):39-56. Doi:10.1016/S0013-7952(01)00099-0

6. Bobet, A. Analytical Solutions for Shallow Tunnels in Saturated Ground. Journal of Engineering Mechanics, 2001, 127(12):1258-1266. Doi:10.1061/(ASCE)0733-9399(2001)127:12(1258)

7. Bobet, A. Effect of pore water pressure on tunnel support during static and seismic loading. Tunnelling & Underground Space Technology, 2003. Doi:10.1016/S0886-7798(03)00008-7

8. Polubarinova-Kochina P Y. Theory of ground water movement. Princeton University Press, 1963. Doi:10.1126/science.139.3557.820

9. Zhang L , Franklin J A . Prediction of water flow into rock tunnels: an analytical solution assuming an hydraulic conductivity gradient. International Journal of Rock Mechanics & Mining Sciences & Geomechanics Abstracts, 1993, 30(1):37-46. Doi:10.1016/0148-9062(93)90174-C

10. Su K , Zhou Y , Wu H , et al. An Analytical Method for Groundwater Inflow into a Drained Circular Tunnel. Ground Water, 2017, 55(5):712-721. Doi:10.1111/gwat.12513

11. Ying H , Zhu C , Gong X . Tide-induced hydraulic response in a semi-infinite seabed with a subaqueous drained tunnel. Acta Geotechnica, 2017. Doi:10.1016/S0886-7798(03)00008-7

12. Zareifard M R . An analytical solution for design of pressure tunnels considering seepage loads. Applied Mathematical Modelling, 2018, 62(OCT.):62-85. Doi:10.1061/(ASCE)IR.1943-4774.0000404

13. EL Tani M. Circular tunnel in a semi-infinite aquifer. Tunnelling & Underground Space Technology Incorporating Trenchless Technology Research, 2003, 18(1):49-55. Doi:10.1016/s0886-7798(02)00102-5

14. Kolymbas D, Wagner P. Groundwater ingress to tunnels – The exact analytical solution. Tunnelling & Underground Space Technology, 2007, 22(1):23-27. Doi:10.1016/j.tust.2006.02.001

15. Park K H , Owatsiriwong A , Lee J G . Analytical solution for steady-state groundwater inflow into a drained circular tunnel in a semi-infinite aquifer: A revisit. Tunnelling and Underground Space Technology incorporating Trenchless Technology Research, 2008, 23(2):206-209. Doi:10.1016/J.TUST.2007.02.004

16. M. Huangfu , Meng-Shu W , Zhong-Sheng T , et al. Analytical solutions for steady seepage into an underwater circular tunnel. Tunnelling & Underground Space Technology Incorporating Trenchless Technology Research, 2010, 25(4):391-396. Doi:10.1016/j.tust.2010.02.002

17. Hu X , Zhang Z , Kieffer S . A real-life stability model for a large shield-driven tunnel in heterogeneous soft soils. Frontiers of Structural and Civil Engineering, 2012, 6(2):176-187. Doi:10.1007/s11709-012-0149-7

18. Rieckh G , Kreuzer W , Waubke H , et al. A 2.5D-Fourier-BEM model for vibrations in a tunnel running through layered anisotropic soil. Engineering Analysis with Boundary Elements, 2012, 36(6):960–967. Doi:10.1016/j.enganabound.2011.12.014

19. Zhang D M , Huang H W , Hu Q F , et al. Influence of multi-layered soil formation on shield tunnel lining behavior. Tunnelling & Underground Space Technology Incorporating Trenchless Technology Research, 2015, 47:123-135. Doi:10.1016/j.tust.2014.12.011

20. Khezri, Nima, Fatahi, et al. Stability assessment of tunnel face in a layered soil using upper bound theorem of limit analysis. Geomechanics and engineering, 2016. Doi:10.12989/GAE.2016.11.4.471

21. Guo P , Wang Y , Gong X ,et al.Analysis of observed performance of a deep excavation straddled by shallowly buried pressurized pipelines and underneath traversed by planned tunnels. Tunnelling and underground space technology, 2023. Doi:10.1061/(ASCE)1090-0241(2005)131:8(1004)

22. B C W Z A , B W W , C H W Y A ,et al.Drainage-induced ground response in a twin-tunnel system through analytical prediction over the seepage field. Underground Space, 2022, 7(3):408-418. Doi:10.1155/2021/6964940

23. Guo P , Gong X , Wang Y ,et al. Minimum cover depth estimation for underwater shield tunnels. Tunnelling and Underground Space Technology, 2021, 115(5):104027. Doi:10.1016/j.tust.2021.104027

24. Guo P , Gong X , Wang Y .Displacement and force analyses of braced structure of deep excavation considering unsymmetrical surcharge effect. Computers and Geotechnics, 2019, 113(SEP.):103102. Doi:10.1016/j.compgeo.2019.103102. Doi:10.1016/j.compgeo.2019.103102

25. Gebiaw A , Engidasew T , Bofu Y ,et al.Streamflow and Sediment Yield Prediction for Watershed Prioritization in the Upper Blue Nile River Basin, Ethiopia.Water, 2017, 9(10):782. Doi:10.3390/w9100782

26. Nune R , George B A , Western A W ,et al.A comprehensive assessment framework for attributing trends in streamflow and groundwater storage to climatic and anthropogenic changes: A case study in the typical semi-arid catchments of Southern India.Hydrological Processes, 2021. Doi:10.1002/hyp.14305

27. Becker P S , Ward A S , Herzog S P ,et al.Testing Hidden Assumptions of Representativeness in Reach-Scale Studies of Hyporheic Exchange.Water Resources Research, 2023. Doi:10.1029/2022WR032718

28. Yuan,Forshay.Using SWAT to Evaluate Streamflow and Lake Sediment Loading in the Xinjiang River Basin with Limited Data.Water, 2019, 12(1):39. Doi:10.3390/w12010039

29. Kumar A .Isotopic Assessment of Groundwater Salinity: A Case Study of the Southwest (SW) Region of Punjab, India.Water, 2022, 14. Doi:10.3390/w14010133

30. Ghosh A , Choi M , Yoon D ,et al.Stream Water Quality Control and Odor Reduction through a Multistage Vortex Aerator: A Novel In Situ Remediation Technology.Water, 2023. Doi:10.3390/w15111982

31. Jesús Godifredo, Ferrer J , Seco A ,et al.Zeolites for Nitrogen Recovery from the Anaerobic Membrane Bioreactor Permeate: Zeolite Characterization.Water, 2023. Doi:10.3390/w15061007

32. Esonien L , Ileikien D , Iteik L ,et al.The Impact of Organic and Intensive Agricultural Activity on Groundwater and Surface Water Quality.Water, 2023. Doi:10.3390/w15061240